Table IV. ^{13}C NMR Spectra[a]

	C_2	C_4	C_5
$Co(ImH)_6^{3+}$	140.58 (−0.45)[b]	122.80 (−0.37)[b]	129.11 (0.04)[b]
$Co(NH_3)_5ImH^{3+}$ [c]	139.64 (−6.00)	121.84 (−8.50)	128.04 (1.71)
N-CH_3-ImH^+ [c]	136.24 (−3.10)	120.54 (−8.20)	124.24 (1.95)
ImH_2^+ [d]	134.59 (−1.64)	120.10 (−2.23)	

[a] The numbers in parentheses are the differences between the acidic and the basic forms, δ(acid) − δ(base). All values are given in ppm. [b] The difference in δ between neutral pH and pH = 9.0. [c] Reference 7. [d] Reference 8.

The absolute values of the pH shift of $Co(ImH)_6^{3+}$ are smaller than for the other imidazole complexes since the shift is a weighted average for the six imidazole groups. Thus, the first ionization corresponds to one-sixth ionization for each one of the imizadole groups. A further confirmation of this assignment comes from the line width data. The signals assigned to C_2 and C_5 are the broad ones. We attribute this broadening to unresolved *J* coupling with the ^{59}Co nucleus. We tested this hypothesis by measuring the ^{59}Co NMR spin-lattice relaxation time as a function of pH. The result, given in Figure 2, shows a sharp drop in the T_1 value of the ^{59}Co nucleus, at pH values of about 6.5, while the first pK_a is pK_1 = 8.65. It is in this pH range where the proton resonances become sharp. The decrease in the ^{59}Co T_1 value at basic pH values is likely to originate from the dissociation of a proton from one of the imidazole ligands. This makes the complex more asymmetric and gives rise to quadrupolar relaxation. Fast proton exchange between the protonated and the deprotonated complexes is responsible for the averaging of T_1, which consequently starts to decrease at a pH where only a small fraction of the complex molecules is ionized.

4. The ^{13}C NMR spectrum of $Co(ImH)_6^{3+}$ is summarized in Table IV. The chemical shifts are similar to those of analogous imidazole compounds. Again, the absolute values of the pH shifts are small since they are averages of one ionized imidazole and five unionized ones. ^{13}C spectra without proton broad-band decoupling resulted in $^1J_{CH}$ values of 216, 198, and 197 Hz for the C_2, C_4, and C_5 carbons, respectively. These values may be compared to $^1J_{CH}$ values of 225 and 203 Hz for C_2 and $C_{4,5}$ of ImH_2^+ and 207 and 191 Hz for the same carbons of ImH.

Discussion

In this paper we report for the first time the preparation of the $Co(ImH)_6^{3+}$ ion and the measurement of some of its properties. As could be expected on the basis of its high symmetry, the ^{59}Co NMR signal of $Co(ImH)_6^{3+}$ is sharp relative to those of other cobalt complexes. Still, since its symmetry is not strictly octahedral, it is not surprising that its T_1 relaxation time is substantially shorter than that of $Co(CN)_6^{3-}$. An immediate use of the sharp ^{59}Co NMR signal of $Co(ImH)_6^{3+}$ was done in the present work, where we optimized the yield of its synthesis by following the concentration of the compound in the reaction mixture in situ. Another application of this signal was the determination of intracellular and extracellular water space in biological systems.[6]

The measurement of the properties of $Co(ImH)_6^{3+}$ enables us to examine the properties of imidazole as a ligand.

1. p*K* Value. The first pK_a value of $Co(ImH)_6^{3+}$, pK_a = 8.65 ± 0.02, is significantly lower than those obtained for $Co(NH_3)_5ImH^{3+}$, α-$Co(trien)(ImH)_2^{3+}$, and β-$Co(trien)(ImH)_2^{3+}$, which are 10.0,[7] 10.1, and about 9.6, respectively[8] (trien = triethylenetetramine). This discrepancy is due in part to the difference in probability of ionization in relation to the number of imidazole ligands in the complex. On this basis alone we expect the first pK_a of $Co(ImH)_6^{3+}$ to be lower than that of $Co(NH_3)_5ImH^{3+}$ by log 6 = 0.78 and those of α- and β-$Co(trien)(ImH)_2^{3+}$ by log 3 = 0.48. Part of the further reduction of the pK_a from the expected value of about 9.2 to the experimental value 8.65 is due to the differences between $Co(ImH)_5^{3+}$ and $Co(NH_3)_5^{3+}$ or $Co(trien)ImH^{3+}$ as ligands of the ionizable imidazole. Another important difference between $Co(ImH)_6^{3+}$ and the other cobalt-imidazole complexes is seen in the proton chemical shifts of the C_2 and C_5 CH groups (see Table II). We suggest this difference results from the magnetic field anisotropies of the neighboring imidazole groups. In the $Co(trien)(ImH)_2^{3+}$ ion, which also contains adjacent imidazole groups, this field anisotropy is averaged out by free rotation of these imidazole groups. We expect this free rotation to be largely restricted in the $Co(ImH)_6^{3+}$ ion.

2. Position in the Spectrochemical Series. The ligand field splitting for $Co(ImH)_6^{3+}$, which was calculated on the basis of its optical spectrum, was found to be lower by 5.4% as compared to that of $Co(NH_3)_6^{3+}$ (see Table II). This difference is the same for two calculation procedures. Thus, imidazole falls below NH_3 in the spectrochemical series. Assuming a value of $f_{ligand} = 1.25$ for NH_3,[9,10] one can estimate $f_{ligand} = 1.18$ for imidazole. The values of the Racah parameters *B* and *C* are smaller than those of $Co(NH_3)_6^{3+}$ by 13% and 5%, respectively, indicating higher covalency for the imidazole as a ligand. In another procedure of calculation, which assumes $C/B = 4.0$, the Racah parameter *B* of $Co(ImH)_6^{3+}$ is smaller than that of $Co(NH_3)_6^{3+}$ by 8.3%. Since the nephelauxetic series is based on such an assumption, we shall use this value for estimating h_{ligand} for imidazole. Thus, since $h_{ligand} = 1.4$ for NH_3,[9] the corresponding value for imidazole is $h_{ligand} = 1.53$. These values position imidazole as a ligand in the spectrochemical and in the nephelauxetic series.

Acknowledgment. The help of the summer students Y. Olshanski, H. Sanderovich and I. Ronen is gratefully acknowledged.

Registry No. $Co(ImH)_6(ClO_4)_3$, 119414-02-7; $Co(ImH_6)^{3+}$, 99774-48-8; $Co(ImH)_6Cl_3$, 119414-03-8; ^{59}Co, 7440-48-4; α-$Co(trien)(ImH)_2^{3+}$, 77341-40-3; β-$Co(trien)(ImH)_2^{3+}$, 77299-00-4; $Co(NH_3)_5ImH^{3+}$, 38716-02-8; *N*-CH_3-ImH^+, 17009-89-1; ImH_2^+, 17009-90-4.

---

(6) Shinar, H.; Navon, G. *FEBS Lett.* **1985**, *193*, 75.

(7) Harrowfield, J. M.; Norris, V.; Sargeson, A. M. *J. Am. Chem. Soc.* **1976**, *98*, 7282.

(8) Rowan, N. S.; Storm, C. B.; Rowan, R. *J. Inorg. Biochem.* **1981**, *14*, 59.

(9) Jørgensen, C. K. *Oxidation Numbers and Oxidation States*; Springer-Verlag: Berlin, Heidelberg, New York, 1969; p 84.

(10) Figgis, B. N. *Introduction to Ligand Fields*; Interscience: New York, 1967; p 244.

Contribution from the Laboratorium voor Anorganische Chemie,
Rijksuniversiteit Groningen, Nijenborgh 16,
9747 AG Groningen, The Netherlands,
and Vakgroep Algemene Chemie, Afdeling Kristal-
en Structuurchemie, Rijksuniversiteit Utrecht,
Padualaan 8, 3584 CH Utrecht, The Netherlands

New Classes of Monomeric and Dimeric Square-Planar Chromium(II) Aryloxides: Syntheses and Structures

Jilles J. H. Edema,[1] Sandro Gambarotta,*[,1] Fre' van Bolhuis,[1] Wilberth J. J. Smeets,[2] and Anthony L. Spek[2]

Received October 5, 1988

The chemistry of low- and medium-valent transition-metal alkoxides has experienced a spectacular growth of interest during the last decade.[3] In contrast to the versatile chemistry discovered for the trivalent molybdenum and tungsten alkoxides,[4] the

---

(1) Rijksuniversiteit Groningen.

(2) Rijksuniversiteit Utrecht.

(3) (a) Mehrotra, R. C. *Adv. Inorg. Chem. Radiochem.* **1983**, *26*, 269. (b) Chisholm, M. H.; Huffman, J. C.; Van Der Sluys, W. G. *J. Am. Chem. Soc.* **1987**, *109*, 2514 and references cited therein. (c) Cotton, F. A.; Diebold, M. P.; Roth, W. J. *Inorg. Chem.* **1985**, *24*, 3509 and references cited therein.

(4) Chisholm, M. H.; Folting, K.; Hammond, C. E.; Hampden-Smith, M. J. *J. Am. Chem. Soc.* **1988**, *110*, 3314 and references cited therein.

Scheme I[a]

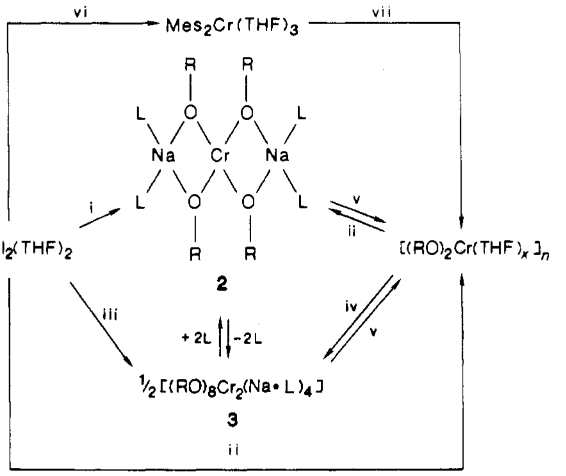

[a]Key: (i) 4RONa, THF; (ii) 2RONa, THF; (iii) 4RONa, THF, Δ, toluene; (iv) 2RONa, thf, Δ, toluene; (v) 18-crown-6; (vi) 2MesMgBr; (vii) 2ROH [R = 2,6-(*t*-Bu)$_2$-4-MePh (**1**), Ph, 2,6-$(CH_3)_2C_6H_3$, β-naphthyl, *i*-Pr].

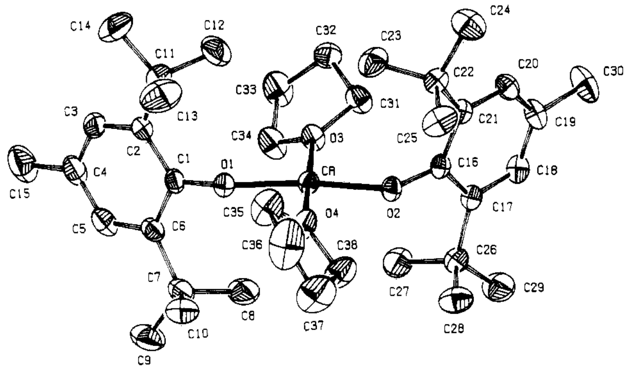

Figure 1. ORTEP view of **1** with thermal ellipsoids drawn at the 30% probability level.

chemistry of the chromium analogues remains almost unknown for both of the oxidation states II and III.[5] Efforts to develop this chemistry might have been discouraged by the low solubility and poor crystallinity reported for these species,[6] probably due to an oligomeric or polymeric nature. More recently, attempts to characterize these complexes, by utilization of extremely bulky alkoxides like tritox [tritox = (*t*-Bu)$_3$CO–], were successful in preventing polymeric aggregation and allowed the isolation of reactive heteroleptic species both monomeric[7] and dimeric.[8] In spite of their ill-defined nature, however, chromium(II) alkoxides[6] are promising starting materials for reactivity studies and in our opinion deserve further synthetic efforts. In this paper we report the syntheses, structural characterization, and chemical behavior of three new types of chromium(II) aryloxides.

Results and Discussion

We found that chromium(II) alkoxides can be conveniently synthesized according to the procedures summarized in Scheme I. As expected, the size of the alkoxide moiety dramatically affects the molecular complexity of the reaction products. Using very bulky substituents, for example, allowed the isolation of the first monomeric chromium(II) alkoxide [2,6-(*t*-Bu)$_2$-4-MePhO]$_2$Cr(THF)$_2$ (**1**). The monomeric nature has been determined by an X-ray diffraction analysis, carried out on a single crystal of **1**. The structure shows the molecule having a slightly distorted square-planar geometry around the chromium atom, with the two aryloxide ligands placed in trans positions (Figure 1). Both aromatic rings are somewhat inclined toward each other [O(1)–Cr–O(2) = 170.44 (9)°], the four *t*-Bu groups being arranged in an eclipsed conformation. The Cr–O bond distances [Cr–O(1) = 1.948 (2) Å, Cr–O(2) = 1.948 (2) Å] are longer than in the previously reported [(*t*-Bu$_3$CO)$_2$CrLiCl(THF)$_2$][7] and [(t-Bu$_3$CO)–Cr–(μ-OCH-*t*-Bu$_2$)]$_2$.[8] The angles subtended at the oxygen atoms are remarkably flattened [Cr–O(1)–C(1) = 147.6 (2)°; Cr–O(2)–C(16) = 139.7 (2)°], probably as result of the high steric congestion.[9] The square-planar arrangement, similar to that observed in the monomeric chromium(II) amide complex [$(Me_3Si)_2N]_2Cr(THF)_2$,[10] is one of the rare cases encountered in the chemistry of Cr(II).[11]

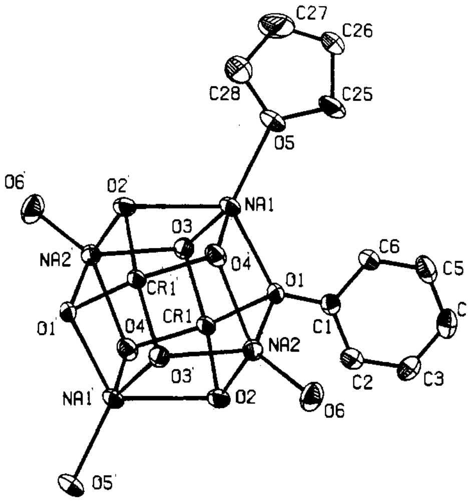

Figure 2. ORTEP view of **3** with thermal ellipsoids drawn at the 50% probability level. For clarity reasons the carbon atoms have been deleted in part. The full picture is available as supplementary material.

The value of the magnetic moment (μ_{eff} = 4.83 μ_B) is in agreement with a high-spin d^4 electronic configuration of the Cr(II) atom in a square-planar coordination geometry (μ_B/Cr calculated spin only for the high-spin d^4 electronic configuration; μ_{eff} = 4.90 μ_B).

In the case of other smaller substituents (R = Me, *i*-Pr, *t*-Bu, Ph, 2,6-dimethylphenyl, β-naphthyl) highly insoluble, pyrophoric solids, probably polymers, have been obtained (Scheme I). However, further reaction of these species with 2 equiv of RONa proceeds smoothly, forming soluble (THF, toluene) and monomeric (RO)$_4$CrNa$_2$(L)$_4$ [R = Ph (a), 2,6-$(CH_3)_2C_6H_3$ (b), β-naphthyl (c); L = THF, py, $^1/_2$ TMEDA] as purple crystalline solids (Scheme I). In the case of {[2,6-$(CH_3)_2C_6H_3O]_4$Cr(Na·TMEDA)$_2$} (**2b**), crystals suitable for X-ray analysis have been obtained.[12]

A common characteristic of these compounds is their ability to lose solvent easily in vacuo, forming greenish gray solids. After recrystallization from toluene containing small amounts of THF

---

(5) (a) Wilkinson, G.; Gillard, R. D.; McCleverty, J. A. *Comprehensive Coordination Chemistry*; Pergamon Press: Oxford, England, 1987; Vol. 3. (b) Cotton, F. A.; Walton, R. A. *Multiple Bonds Between Metal Atoms*; Wiley: New York 1982; and references cited therein. (c) Bochman, M.; Wilkinson, G.; Yong, B. G.; Hursthouse, M. B.; Malik, K. M. A. *J. Chem. Soc., Dalton Trans.* **1980**, 1863. (d) Bochman, M.; Wilkinson, G.; Yong, B. G.; Hursthouse, M. B.; Malik, K. M. A. *J. Chem. Soc., Dalton Trans.* **1980**, 901.

(6) Horvath, B.; Horvath, E. G. *Z. Anorg. Allg. Chem.* **1979**, *457*, 51.

(7) Hvoslef, J.; Hope, H.; Murray, B. D.; Power, P. P. *J. Chem. Soc., Chem. Commun.* **1983**, 1438.

(8) Murray, B. D.; Hope, H.; Power, P. P. *J. Am. Chem. Soc.* **1985**, *107*, 169.

(9) Although unlikely, a partial contribution from a O→Cr π-bonding mechanism cannot be excluded.

(10) Bradley, D. C.; Hursthouse, M. B.; Newing, C. W.; Welch, G. *J. Chem. Soc., Chem. Commun.* **1972**, 567.

(11) (a) Eremenko, I. L.; Pasynskii, A. A.; Kalinnikov, V. T.; Aleksandrov, G. G.; Struchkov, Y. T. *Inorg. Chim. Acta* **1981**, *54*, L85. (b) Hermes, A. R.; Morris, J. R.; Girolami, G. S. *Organometallics* **1988**, *7*, 2372. (c) Dapporto, M.; Mani, F.; Mealli, C. *Inorg. Chem.* **1978**, *17*, 1323. (d) Larkworthy, L. F.; Povey, D. C.; Sandell, B. *Inorg. Chim. Acta* **1984**, *83*, L29. (e) Scheidt, W. R.; Reed, C. A. *Inorg. Chem.* **1978**, *17*, 710.

(12) Edema, J. J. H.; Gambarotta, S.; van Bolhuis, F.; Spek, A. L. X-ray structure, *J. Am. Chem. Soc.*, in press.

or py, emerald green crystals of $(RO)_8Cr_2(Na{\cdot}L)_4$ (R = Ph, β-naphthyl; L = THF, py) have been isolated in good yield (Scheme I).

In the case of $(PhO)_8Cr_2(Na{\cdot}THF)_4$ (**3**), the structure has been clarified by an X-ray diffraction analysis. The geometry of the molecule can be described in terms of a distorted octahedron positioned on an inversion center, with two Cr atoms occupying the apical positions and the four Na sited on the equatorial vertices (Figure 2). The eight aryloxide groups are capping the faces of the octahedron with η^3-OR groups [Cr–O = 1.985–2.000Å, Na–O = 2.348–2.532 Å]. The Cr atoms are slightly outside the plane described by the four closest oxygen atoms (distance from the plane is 0.251 Å) resulting in distorted-square-planar coordination geometry of the transition metal. The Na atoms are pentacoordinated, the fifth coordination site being occupied by one molecule of THF.

Linear dependence of the magnetic susceptibility on $1/T$, in agreement with the Curie–Weiss law, has been found in the range 50–298 K. The value of the magnetic moment of **3** (μ_{eff} = 2.84 μ_B) could be accounted for by a low-spin (S = 1) d^4 electronic configuration (μ_B/Cr calculated spin only for a low-spin (S = 1) d^4 electronic configuration; μ_{eff} = 2.83 μ_B). However, strong direct antiferromagnetic exchange, the presence of which is suggested by the highly negative value of Θ (Θ = −115 K), is likely to be responsible for the low value of μ_{eff}, as may be ligand-mediated superexchange.[13]

In spite of the remarkable structural similarity with the previously reported $R_8Cr_2(Li{\cdot}L)_4$ (R = CH_3, $^1/_2$ $CH_2(CH_2)_2CH_2$; L = THF, Et_2O) complexes[14,15] (which contain a supershort quadruple Cr–Cr bond),[5b] the long Cr···Cr intermetallic distance [3.622 (1) Å] in the present case rules out any possible bonding between the two chromium atoms. Calculations carried out on the basis of purely geometrical considerations excluded as unrealistic the possibility of ascribing the absence of the Cr–Cr supershort quadruple bond simply to the increased size of the alkali-metal cation.[16] The different number of orbitals and electrons used by η^3-OR for bonding, compared to η^3-CH_3, are in our opinion more likely to be responsible for this surprising discrepancy.

The Lewis acidity of the alkali-metal cation plays an important role in the assemblage of the dimeric structure. In fact, simple addition of 18-crown-6 to solutions of both **2** and **3** causes Na abstraction from the Cr units, forming the initial polymeric $[(RO)_2Cr(THF)_x]_n$ (Scheme I). Finally, addition/removal of coordinating solvents (THF, py) to/from the coordination sphere of Na allows the transformation of the purple monomeric (**2**) and the dimeric green (**3**) complexes into each other (Scheme I).

Experimental Section

All the operations were performed under dry nitrogen with use of standard Schlenk techniques, or in a nitrogen-filled drybox (Braun MB-200). $CrCl_2(THF)_2$[17] and $Mes_2Cr(THF)_3$[18] have been prepared according to published methods. Solvents were dried and distilled in accordance with standard procedures. Infrared spectra were recorded on a Unicam SP3-300 instrument; Nujol mulls were prepared in the drybox. Elemental analyses were carried out at the Chemistry Department of the State University of Groningen. Magnetic measurements were determined on an MB 4 Oxford Gouy balance interfaced with an Apple II computer. Calculations of the μ_{eff} values were carried out by standard methods.

Table I. Data Collection and Structure Refinement Information

	1	3
space group	$P2_1/n$	$P2_1/n$
cryst syst	monoclinic	monoclinic
a, Å	10.218 (1)	13.680 (5)
b, Å	23.308 (4)	16.078 (3)
c, Å	16.033 (1)	14.009 (4)
β, deg	99.96 (1)	95.59 (2)
V, Å^3	3760.9 (8)	3066.6 (5)
Z	4	2
ρ(calcd), g cm^{-3}	1.121	1.331
cryst dimens, mm	0.25 × 0.25 × 0.75	0.45 × 0.40 × 0.50
chem formula	$C_{38}H_{62}O_4Cr$	$C_{64}H_{72}O_{12}Na_4Cr_2$
fw	634.90	1229.23
λ(Mo Kα), Å	0.71073	0.71073
T, K	295	130
scanning range	$1.74 \leq 2\theta \leq 50.0$	$2 \leq 2\theta \leq 50$
scan mode	ω–2θ	ω–2θ
abs coeff (μ), cm^{-1}	3.3	4.30
R	0.053	0.047
R_w	0.048	0.059

Table II. Positional Parameters and Their Estimated Standard Deviations for **1**

atom	x	y	z	U(eq), Å^2
Cr	0.64035 (6)	0.09508 (2)	0.28531 (3)	0.0433 (2)
O(1)	0.6629 (2)	0.07863 (9)	0.1695 (1)	0.0525 (9)
O(2)	0.6123 (2)	0.09787 (9)	0.4023 (1)	0.0467 (8)
O(3)	0.7086 (2)	0.17985 (9)	0.2840 (1)	0.0525 (9)
O(4)	0.5650 (3)	0.0120 (1)	0.2861 (1)	0.064 (1)
C(1)	0.7205 (4)	0.0929 (2)	0.1039 (2)	0.048 (1)
C(2)	0.6498 (4)	0.1251 (2)	0.0352 (2)	0.056 (1)
C(3)	0.7178 (5)	0.1426 (2)	−0.0271 (2)	0.071 (2)
C(4)	0.8477 (5)	0.1290 (2)	−0.0291 (3)	0.074 (2)
C(5)	0.9114 (4)	0.0948 (2)	0.0344 (2)	0.069 (2)
C(6)	0.8523 (4)	0.0751 (2)	0.1000 (2)	0.053 (2)
C(7)	0.9285 (4)	0.0330 (2)	0.1657 (2)	0.063 (2)
C(8)	0.9535 (5)	0.0581 (2)	0.2558 (3)	0.093 (2)
C(9)	1.0654 (4)	0.0171 (2)	0.1455 (3)	0.096 (2)
C(10)	0.8489 (5)	−0.0225 (2)	0.1663 (3)	0.085 (2)
C(11)	0.5029 (4)	0.1396 (2)	0.0294 (3)	0.072 (2)
C(12)	0.4762 (6)	0.1778 (2)	0.0994 (3)	0.125 (3)
C(13)	0.4228 (5)	0.0852 (2)	0.0312 (4)	0.126 (3)
C(14)	0.4423 (7)	0.1693 (3)	−0.0527 (3)	0.145 (3)
C(15)	0.9188 (6)	0.1507 (2)	−0.0983 (3)	0.118 (3)
C(16)	0.6042 (4)	0.1364 (1)	0.4631 (2)	0.042 (1)
C(17)	0.7159 (4)	0.1469 (1)	0.5268 (2)	0.045 (1)
C(18)	0.7068 (4)	0.1919 (2)	0.5825 (2)	0.053 (2)
C(19)	0.5950 (4)	0.2246 (2)	0.5805 (2)	0.058 (2)
C(20)	0.4840 (4)	0.2102 (2)	0.5222 (2)	0.054 (2)
C(21)	0.4831 (3)	0.1661 (2)	0.4652 (2)	0.043 (1)
C(22)	0.3517 (4)	0.1492 (2)	0.4082 (2)	0.051 (1)
C(23)	0.3541 (4)	0.1574 (2)	0.3135 (2)	0.084 (2)
C(24)	0.2338 (4)	0.1849 (2)	0.4258 (3)	0.088 (2)
C(25)	0.3217 (5)	0.0865 (2)	0.4230 (3)	0.080 (2)
C(26)	0.8432 (4)	0.1113 (2)	0.5359 (2)	0.052 (1)
C(27)	0.9129 (4)	0.1197 (2)	0.4605 (3)	0.089 (2)
C(28)	0.8109 (5)	0.0477 (2)	0.5448 (3)	0.083 (2)
C(29)	0.9458 (5)	0.1271 (2)	0.6130 (3)	0.093 (2)
C(30)	0.5943 (5)	0.2755 (2)	0.6406 (3)	0.093 (2)
C(31)	0.6756 (4)	0.2283 (1)	0.3340 (2)	0.066 (2)
C(32)	0.6809 (4)	0.2789 (2)	0.2763 (2)	0.071 (2)
C(33)	0.7870 (5)	0.2634 (2)	0.2264 (3)	0.096 (2)
C(34)	0.8082 (4)	0.2001 (2)	0.2374 (3)	0.075 (2)
C(35)	0.4688 (5)	−0.0130 (2)	0.2199 (3)	0.093 (2)
C(36)	0.4323 (7)	−0.0687 (2)	0.2549 (3)	0.141 (4)
C(37)	0.5408 (7)	−0.0836 (2)	0.3219 (3)	0.125 (3)
C(38)	0.5977 (5)	−0.0281 (2)	0.3541 (3)	0.091 (2)

$[(2,6\text{-}(t\text{-}Bu)_2\text{-}4\text{-}MeC_6H_2O)_2Cr(THF)_2]$ (1). Neat 2,6-$(t\text{-}Bu)_2$-4-MeC_6H_2OH (0.66 g, 3.01 mmol) was added to a solution of 0.77 g of $Mes_2Cr(THF)_3$ (1.51 mmol) in 20 mL of THF. The resulting solution was gently heated until the color changed to blue. After 12 h of stirring, the mixture was evaporated to dryness. Recrystallization of the residual blue solid from heptane gave 0.92 g of blue crystalline solid (1.4 mmol, 91% yield). Anal. Calcd (found) for $C_{38}H_{62}O_4Cr$: C, 71.90 (71.95); H, 9.80 (10.00); Cr, 8.20 (7.98). IR (Nujol mull, KBr, cm^{-1}): 1405 (s), 1350 (w), 1260 (s), 1250 (m), 1225 (w), 1210 (w), 1190 (w), 1150 (w), 1105 (w), 1005 (s), 905 (w), 870 (w), 855 (m), 825 (m), 800 (w), 585 (w), 710 (w), 535 (s). μ_{eff} = 4.68 μ_B.

$[(2,6\text{-}Me_2C_6H_3O)_4Cr(Na{\cdot}TMEDA)_2]{\cdot}tol$ (2) (tol = Toluene). In a standard experiment, the suspension obtained upon treatment of 2,6-$Me_2C_6H_3OH$ (0.25 g, 2.1 mmol) with NaH (0.053 g, 2.2 mmol) in THF (10 mL) was reacted with $(2,6\text{-}Me_2C_6H_3O)_2Cr$ (0.3 g, 1.0 mmol). The

---

[13] Mabbs, F. E.; Machin, D. J. *Magnetism and Transition Metal Complexes*; Chapman and Hall: London, 1973.

[14] Krausse, J.; Mark, G.; Schodl, G. *J. Organomet. Chem.* **1970**, *21*, 159.

[15] Krausse, J.; Schodl, G. *J. Organomet. Chem.* **1971**, *27*, 59.

[16] Ionic radii 0.95 and 0.60 Å for Na and Li, respectively: Pauling, L. *The Nature of the Chemical Bond*; Cornell University Press: Ithaca, NY, 1967.

[17] Kohler, F. H.; Prossdorf, W. *Z. Naturforsch.* **1977**, *32B*, 1026.

[18] Tsutsui, M.; Zeiss, H. *J. Am. Chem. Soc.* **1960**, *82*, 6255.

Table III. Positional Parameters and Their Estimated Standard Deviations for **3**

atom	*x*	*y*	*z*	*B*, Å^2
Cr	0.95337 (5)	0.08155 (4)	0.91877 (4)	1.88 (1)
Na(1)	1.1198 (1)	−0.0517 (1)	0.8739 (1)	2.07 (3)
Na(2)	0.8630 (1)	−0.0968 (1)	0.9215 (1)	2.11 (3)
O(1)	0.9571 (2)	−0.0063 (2)	0.8192 (2)	1.98 (6)
O(2)	0.8209 (2)	0.0422 (2)	0.9482 (2)	2.19 (6)
O(3)	1.0964 (2)	0.1002 (2)	0.9134 (2)	2.32 (6)
O(4)	0.9663 (2)	0.1458 (2)	1.0404 (2)	2.15 (6)
O(5)	1.2334 (2)	−0.0939 (2)	0.7763 (2)	3.06 (7)
O(6)	0.7412 (2)	−0.1870 (2)	0.8782 (2)	3.25 (8)
C(1)	0.9064 (3)	−0.0160 (3)	0.7330 (3)	1.82 (8)
C(2)	0.8056 (3)	−0.0030 (4)	0.7166 (3)	3.3 (1)
C(3)	0.7562 (4)	−0.0162 (4)	0.6269 (4)	4.3 (1)
C(4)	0.8054 (4)	−0.0416 (3)	0.5501 (3)	3.3 (1)
C(5)	0.9054 (4)	−0.0540 (3)	0.5651 (3)	3.01 (1)
C(6)	0.9553 (3)	−0.0411 (3)	0.6544 (3)	2.5 (1)
C(7)	0.7350 (3)	0.0841 (3)	0.9431 (3)	2.03 (8)
C(8)	0.7304 (3)	0.1705 (3)	0.9465 (3)	2.6 (1)
C(9)	0.6407 (4)	0.2110 (3)	0.9423 (3)	3.3 (1)
C(10)	0.5533 (3)	0.1662 (4)	0.9354 (3)	3.4 (1)
C(11)	0.5567 (3)	0.0814 (4)	0.9303 (3)	3.3 (1)
C(12)	0.6463 (3)	0.0396 (3)	0.9336 (3)	2.6 (1)
C(13)	1.1481 (3)	0.1212 (3)	0.8402 (3)	1.85 (8)
C(14)	1.1040 (3)	0.1386 (3)	0.7489 (3)	2.31 (9)
C(15)	1.1599 (4)	0.1615 (3)	0.6752 (3)	3.2 (1)
C(16)	1.2606 (4)	0.1665 (4)	0.6913 (3)	3.8 (1)
C(17)	1.3060 (3)	0.1455 (4)	0.7808 (3)	3.7 (1)
C(18)	1.2509 (3)	0.1231 (3)	0.8550 (3)	2.9 (1)
C(19)	0.9831 (3)	0.2260 (3)	1.0584 (3)	1.88 (9)
C(20)	1.0164 (3)	0.2515 (3)	1.1527 (3)	2.24 (9)
C(21)	1.0334 (3)	0.3337 (3)	1.1740 (4)	3.2 (1)
C(22)	1.0173 (4)	0.3939 (3)	1.1051 (4)	3.8 (1)
C(23)	0.9850 (4)	0.3701 (3)	1.0119 (4)	3.7 (1)
C(24)	0.9701 (3)	0.2869 (3)	0.9886 (3)	2.7 (1)
C(25)	1.2197 (6)	−0.1169 (7)	0.6755 (6)	4.0 (2)
C(25′)	1.2275 (9)	−0.073 (1)	0.6727 (9)	4.0 (3)
C(26)	1.3235 (6)	−0.1333 (7)	0.6485 (6)	3.9 (2)
C(26′)	1.3339 (8)	−0.071 (1)	0.6454 (9)	3.9 (3)
C(27)	1.3890 (4)	−0.0993 (6)	0.7246 (5)	7.3 (2)
C(28)	1.3362 (4)	−0.1000 (4)	0.8118 (4)	4.5 (1)
C(29)	0.7279 (4)	−0.2621 (4)	0.9316 (4)	3.8 (1)
C(30)	0.6349 (5)	−0.2990 (4)	0.8859 (4)	5.2 (2)
C(31)	0.6471 (8)	−0.2798 (6)	0.7802 (5)	9.4 (3)
C(32)	0.7005 (5)	−0.2005 (5)	0.7820 (4)	5.8 (2)

solid dissolved, forming a purple solution. After evaporation to dryness and recrystallization of the resulting purple solid from toluene/TMEDA (10:1), purple crystals of **2** separated on cooling (0.42 g, 0.46 mmol, 46% yield). Anal. Calcd (found) for $C_{51}H_{76}O_4N_4Na_2Cr$: C, 67.55 (67.31); H, 8.39 (8.51); Cr, 5.71 (5.74); N, 6.18 (6.11); Na, 5.08 (5.39). IR (Nujol mull, KBr, cm^{-1}): 1585 (s), 1405 (s), 1260 (m), 1250 (m), 1210 (m), 1185 (m), 1160 (w), 1150 (w), 1110 (w), 1070 (s), 1020 (w), 1005 (s), 925 (m), 825 (s), 725 (s), 670 (s), 585 (m), 510 (s), 450 (m). μ_{eff} = 3.45 μ_B.

[(OPh)$_8$Cr$_2$(Na·THF)$_4$] (3). In a standard experiment, a suspension of PhONa in THF (75 mL) [obtained by reacting 0.80 g of NaH (33.3 mmol) with 3.14 g of phenol (33.4 mmol)], was reacted with $CrCl_2(THF)_2$ (2.20 g, 8.24 mmol). The resulting purple mixture was stirred for 1.5 h, filtered, and cooled at −30 °C. The well-formed purple crystals, which lost solvent under an N_2 stream, were pumped in vacuo, forming a green pyrophoric solid. Green crystals were obtained upon recrystallization from toluene/THF mixtures (4:1) (3.74 g, 3.0 mmol, 74% yield). Anal. Calcd (found) for $C_{64}H_{72}O_{12}Cr_2Na_4$: C, 61.99 (62.42); H, 6.45 (5.99); Cr, 8.38 (7.94); Na, 7.42 (7.30). IR [Nujol mull, KBr, cm^{-1}]: 1590 (s) 1485 (s) 1270 (s) 1160 (m) 1050 (m) 990 (w) 840 (m) 835 (w) 760 (s) 695 (s) 885 (s). μ_{eff} = 2.84 μ_B.

X-ray Crystallographic Studies

All X-ray data were collected on Enraf-Nonius CAD-4F fully automatic diffractometers equipped with locally modified low-temperature devices. Scaling factors and Lorentz and polarization corrections were applied to the data. No absorption corrections were necessary. Details on crystal data and refinement are given in Table I.

Crystal Data for $C_{38}H_{62}O_4Cr$ (1). M_R = 634.90, monoclinic, space group $P2_1/n$, a = 10.218 (1) Å, b = 23.308 (4) Å, c = 16.033 (1) Å, β = 99.96 (1)°, V = 3760.9 (8) Å^3, Z = 4, D_c = 1.121 g/cm^{-3}, $F(000)$ = 1384, Zr-filtered Mo Kα radiation with λ = 0.71073 Å, and μ(Mo Kα) = 3.3 cm^{-1}. Intensities of 13955 reflections were collected ($2\theta_{max}$ = 50°, $\omega/2\theta$ scan) at 295 K. A total of 3981 independent reflections with $I > 2.5\sigma(I)$ were used in the structure determination. The structure was solved by direct methods (SHELXS86) and refined by blocked full-matrix least-squares techniques (SHELX76) to R = 0.0533, (R_w = 0.0478). All of the hydrogen atoms were introduced at calculated positions with C–H = 0.98 Å and included in the refinement with three isotropic thermal parameters. Positional and thermal parameters are given in Table II.

Table IV. Selected Bond Distances (Å) and Angles (deg)

complex **1**		complex **3**	
Cr–O(1)	1.948 (2)	Cr–O(1)	1.990 (3)
Cr–O(3)	2.097 (2)	Na(2)–O(1)	2.488 (3)
O(1)–Cr–O(2)	170.44 (9)	Na(2)–O(6)	2.247 (4)
O(2)–Cr–O(3)	94.73 (9)	O(1)–Cr–O(2)	90.3 (1)
O(3)–Cr–O(4)	177.8 (1)	O(1)–Na(2)–O(2)	71.6 (1)
Cr–O(1)–C(1)	147.6 (2)	O(1)–Na(2)–O(6)	129.3 (1)
Cr–O(2)–C(16)	139.7 (2	Cr···Cr′	3.622 (1)
		Cr···Na(2)	3.120 (7)
		Na(1)···Na(2)	3.711 (2)

Crystal Data for $(C_{32}H_{36}O_6Na_2Cr)_2$ (3). M_R = 1229.23, monoclinic, space group $P2_1/n$, a = 13.680 (5) Å, b = 16.078 (3) Å, c = 14.009 (4) Å, β = 95.59 (2)°, V = 3066.6 (5) Å^3, Z = 2, D_c = 1.33 g/cm^3, and $F(000)$ = 1288. Data were measured ($2\theta_{max}$ = 50°) at low temperature (130 K) by using graphite-filtered Mo Kα radiation (λ = 0.71073 Å) and scan type θ–2θ. A total of 4171 independent reflections with $I > 3\sigma(I)$ were used in the structure determination. The structure was partly solved by direct methods. The positions of the remaining atoms were revealed from succeeding Fourier difference maps. Block-diagonal least-squares techniques were used in the refinement. All the non-hydrogen atom positions were refined anisotropically. All the hydrogen atoms were introduced at calculated positions with C–H = 0.98 Å and included in the refinement with three isotropic thermal parameters. The final R values converged to R = 0.047 (R_w = 0.059). Positional and thermal parameters are given in Table III.

Acknowledgment. This work was supported in part (W.J.J.S. and A.L.S.) by the Netherlands Foundation for Chemical Research (SON) with financial aid from the Netherlands Organization of Scientific Research (NWO).

Registry No. **1**, 119365-62-7; **2**, 119010-41-2; **3**, 119010-44-5; $CrCl_2(THF)_2$, 15604-50-9; $MeS_2Cr(THF)_3$, 15604-48-5; $(PhO)_4CrNa_2(THF)_4$, 119327-38-7; $(PhO)_4CrNa_2(py)_4$, 119327-40-1; $(PhO)_4CrNa_2(^1/_2TMEDA)_4$, 119327-42-3; $[2,6-(CH_3)_2C_6H_3O]_4CrNa_2(THF)_4$, 119327-43-4; $[2,6-(CH_3)_2C_6H_3O]_4CrNa_2(py)_4$, 119327-44-5; ($\beta$-naphthyl-O)$CrNa_2(THF)_4$, 119327-45-6; ($\beta$-naphthyl-O)$CrNa_2(py)_4$, 119327-46-7; ($\beta$-naphthyl-O)$CrNa_2(^1/_2TMEDA)_4$, 119327-47-8; $(PhO)_8Cr(Na\cdot py)_4$, 119010-47-8; (β-naphthyl-O)$_8Cr_2(Na\cdot THF)_4$, 119038-53-8; (β-naphthyl-O)$_8Cr_2(Na\cdot py)_4$, 119327-48-9.

Supplementary Material Available: Complete listings of crystal data, positional atomic parameters, thermal parameters, and bond distances and angles for **1** and **3** and torsion angles for **1** and an ORTEP drawing for **3** showing all the non-hydrogen atoms with the labeling scheme (17 pages); listings of observed and calculated structure factors for complexes **1** and **3** (61 pages). Ordering information is given on any current masthead page.

Contribution from the Department of Physical
and Inorganic Chemistry, University of Western Australia,
Nedlands, WA 6009, Australia

1:1 Adducts of Lead(II) Thiocyanate with 1,10-Phenanthroline and 2,2′:6′,2″-Terpyridine[†]

Lutz M. Engelhardt, Brenda M. Furphy,
Jack McB. Harrowfield,* Jennifer M. Patrick,
and Allan H. White

Received August 3, 1988

The chemistry of polypyridyl and related aza-aromatic ligands is currently of considerable interest, particularly as knowledge

---

[†] Lewis-Base Adducts of Lead(II) Compounds. 5. Part 4: ref 8.

0020-1669/89/1328-1410$01.50/0 © 1989 American Chemical Society